JOURNAL OF BACTERIOLOGY, Sept. 2006, p. 6277–6285 Vol. 188, No. 17
0021-9193/06/$08.00+0 doi:10.1128/JB.00591-06

The Highly Efficient Translation Initiation Region from the *Escherichia coli rpsA* Gene Lacks a Shine-Dalgarno Element

Patricia Skorski,[1] Prune Leroy,[2]† Olivier Fayet,[3] Marc Dreyfus,[1] and Sylvie Hermann-Le Denmat[1]*

Laboratoire de Génétique Moléculaire, École Normale Supérieure-CNRS UMR 8541, Paris, France[1]; Génétique Moléculaire, Evolutive, et Médicale, INSERM U571, Université Paris V, Paris, France[2]; and Laboratoire de Microbiologie et Génétique Moléculaires, Université Paul Sabatier-CNRS UMR 5100, Toulouse, France[3]

Received 26 April 2006/Accepted 26 May 2006

The translational initiation region (TIR) of the *Escherichia coli rpsA* gene, which encodes ribosomal protein S1, shows a number of unusual features. It extends far upstream (to position −91) of the initiator AUG, it lacks a canonical Shine-Dalgarno sequence (SD) element, and it can fold into three successive hairpins (I, II, and III) that are essential for high translational activity. Two conserved GGA trinucleotides, present in the loops of hairpins I and II, have been proposed to form a discontinuous SD. Here, we have tested this hypothesis with the "specialized ribosome" approach. Depending upon the constructs used, translation initiation was decreased three- to sevenfold upon changing the conserved GGA to CCU. However, although chemical probing showed that the mutated trinucleotides were accessible, no restoration was observed when the ribosome anti-SD was symmetrically changed from CCUCC to GGAGG. When the same change was introduced in the SD from a conventional TIR as a control, activity was stimulated. This result suggests that the GGA trinucleotides do not form a discontinuous SD. Others hypotheses that may account for their role are discussed. Curiously, we also find that, when expressed at moderate level (30 to 40% of total ribosomes), specialized ribosomes are only twofold disadvantaged over normal ribosomes for the translation of bulk cellular mRNAs. These findings suggest that, under these conditions, the SD–anti-SD interaction plays a significant but not essential role for the synthesis of bulk cellular proteins.

In both prokaryotes and eukaryotes, mRNAs are translated with different efficiencies depending upon their sequence and structure. In *Escherichia coli*, the mRNA region important for translation initiation (translation initiation region [TIR]) usually spans only a few tens of nucleotides bracketing the translation start (11). Besides the initiation codon itself (most commonly AUG [83%] and less frequently GUG [14%] or UUG [3%] [25]), the TIR generally contains a Shine-Dalgarno sequence (SD) located 4 to 15 bp upstream of it. The SD is a stretch of nucleotides with variable complementarity to the 3′ end (. . .ACCUCCUUA-3′) of 16S rRNA, the RNA from the 30S ribosomal subunit. The importance of the SD–anti-SD (ASD) pairing has been conclusively demonstrated with the "specialized ribosome" approach, where the expression of a specific target mRNA is first depressed by mutations within the SD and then restored by compensatory mutations in the ASD (17, 20). However, overall, the strength of the SD correlates only weakly with the efficiency of translation (23). Obviously, other determinants within the TIR must contribute to this efficiency (see references 14 and 22 for reviews).

Two of these determinants have been particularly well characterized. One is the binding site for ribosomal protein S1. Many TIRs carry short U- or A/U-rich nucleotide stretches upstream of the initiation codon that have a positive effect on translation, presumably because they bind protein S1 (4, 37, 44). Another, particularly important determinant of translation initiation is mRNA structure. Structure can inhibit translation by hampering the access of the 30S ribosomal subunit to its binding site (ribosome binding site [RBS]) within the TIR (9, 29). The affinity of the 30S subunit for the RBS is large enough to iron out weak mRNA structures, and indeed one of the roles of the SD-ASD interaction might be to provide energy for this process (8, 40), but beyond a stability threshold an inverse correlation exists between structure stability and translation efficiency (9). However, secondary structures within the RBS do not invariably depress translation; in some cases, their effect is neutral, presumably because they do not compromise the interaction between the mRNA and the 30S subunit. Such noninhibitory structures have been found upstream of the SD (36), between the SD and the initiation codon (16, 30, 33), or downstream of the start codon (33). That secondary structures can be accommodated by the ribosome illustrates the fact that the mRNA does not necessarily bind continuously to the ribosomal mRNA track, a feature recently documented by structural studies (21).

The TIR of the *E. coli rpsA* gene, encoding ribosomal protein S1, illustrates an unusual situation where the local mRNA structure is not only noninhibitory but even instrumental to translation initiation (3). This TIR is extremely efficient despite of the absence of a canonical SD element: it carries only a vestigial SD (GAAG) that is not essential for activity. Among its unique characteristics is its length—it extends as far as 91 nucleotides (nt) upstream from the AUG start codon–and its structure. Indeed, it can fold into three successive hairpins (named I, II, and III from 5′ to 3′) (Fig. 1) separated by two A/U-rich single-stranded regions (named ss1 and ss2)

* Corresponding author. Mailing address: Laboratoire de Génétique Moléculaire, École Normale Supérieure-CNRS UMR 8541, 46 rue d'Ulm, 75230 Paris Cedex 05, France. Phone: (33) 1 44 32 35 41. Fax: (33) 1 44 42 39 41. E-mail: shermann@biologie.ens.fr.

† Present address: Department of Cell and Molecular Biology, Molecular Biology Programme, Biomedical Center, Box 596, Husargatan 3, SE-751 24 Uppsala, Sweden.

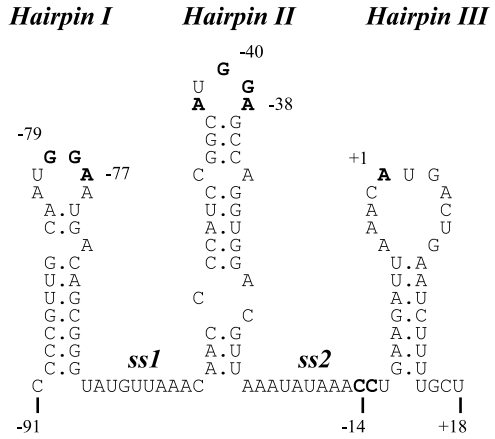

Nomenclature	LoopI	LoopII	ss2	+1
WT (loopI+II^{WT},AUG)	**GGA**	**AUGGA**	**ACCU**	**AUG**
loopI+II^{mut},AUG	CCU	UUCUU	-	-
loopI+II^{WT},GUG	-	-	-	GUG
loopI+II^{mut},GUG	CCU	UUCCU	-	GUG
loopI+II^{WT},UUG	-	-	-	UUG
loopI+II^{mut},UUG	CCU	UUCCU	-	UUG
loopI+II^{WT},UUG, ΔCC	-	-	AU	UUG
loopI+II^{mut},UUG, ΔCC	CCU	UUCCU	AU	UUG
loopI+II^{WT},UUG, CC->AU	-	-	AAUU	UUG
loopI+II^{mut},UUG, CC->AU	CCU	UUCCU	AAUU	UUG

FIG. 1. (Top) Secondary structure of *E. coli rpsA* TIR and site-directed mutations introduced in the sequence. The TIR is folded in three successive hairpins (I, II, and III) separated by single-stranded regions (ss1 and ss2), as determined by chemical probing experiments and phylogenetic comparisons (3). The online *mfold* (version 3.1) computer program (26, 45) predicts energy parameters of −10.8, −11.4, and −2.7 kcal/mol for hairpins I, II, and III, respectively. The sequence is numbered from the first base of the initiator codon; mutated positions are in boldface. (Bottom) For each mutated *rpsA* TIR used in this work, the combined mutations are listed according to their position in the sequence. A dash indicates a sequence identical to the wild-type (WT) sequence.

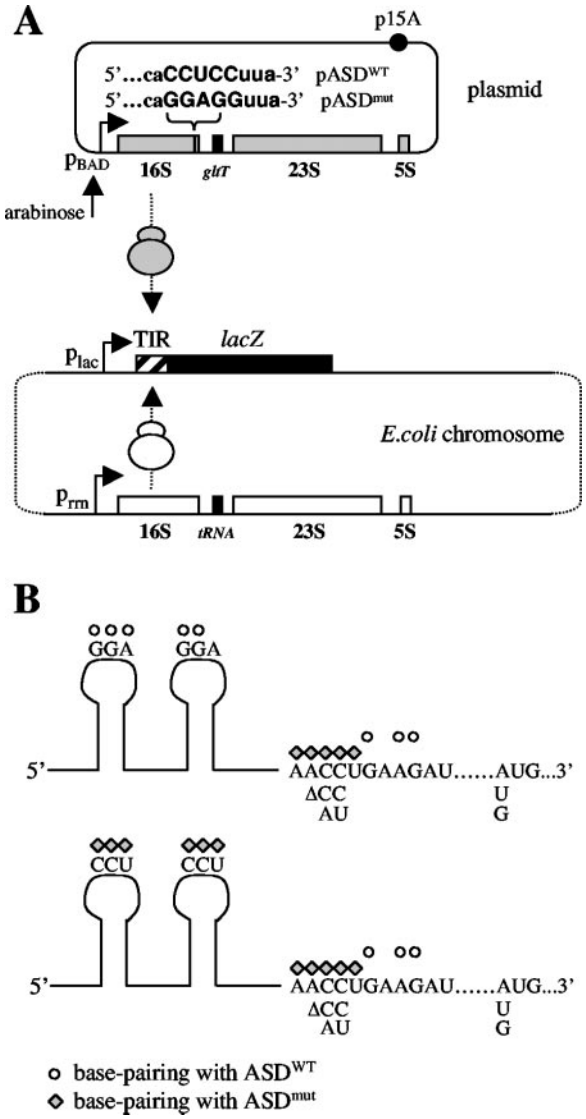

FIG. 2. (A) The genetic system used here. Plasmid and *E. coli* chromosomes are schematically shown as large rectangles. The plasmid-borne *rrnB* operon (gray boxes) is under control of the arabinose-inducible P_{BAD} promoter. Sequences of the anti-SD borne by the pASD^{WT} and pASD^{mut} plasmids are indicated. Only one of the seven chromosomal *rrn* operons is represented (open boxes), along with the IPTG-inducible *lacZ* chromosomal fusion used as the translational reporter (hatched and closed boxes). (B) Schematic representation of the *rpsA* TIR, indicating possible base pairings with the wild-type (ASD^{WT}) or specialized (ASD^{mut}) ASD. The upper drawing corresponds to the wild-type TIR, whereas in the lower one the GGA motifs in loops I and II are changed to CCU. Additional mutations introduced in each TIR are indicated below the sequence. For clarity, the weak hairpin III is represented unfolded.

(2, 3). Hairpins I and II are very stable, whereas hairpin III, which contains the initiator codon in the apical loop and the vestigial SD in the stem, is less so (Fig. 1). This phylogenetically conserved structure is required for the high translational activity of the TIR in *E. coli*, as well as for the autoregulation exerted by the ribosomal protein S1 on its own translation (3, 41). Presumably, the specific folding of the *rpsA* TIR generates an optimal spatial arrangement of sequence elements that interact with the 30S ribosomal subunit (3).

Two conserved GGA motifs present in apical loops of hairpins I and II (Fig. 1) presumably stand among such elements. These motifs, which are individually necessary for high translation activity, are separated by 39 nt from each other and by 79 and 40 nt, respectively, from the initiation codon (Fig. 1) (3). One intriguing possibility is that, in spite of this large separation, the structure of the TIR brings them close enough to each other and to the initiation codon to form a discontinuous SD. Overall this discontinuous SD (GGA.GGA) would show a much higher complementarity to the anti-SD than the vestigial SD-like element (Fig. 2B). Here, we have tested this hypothesis with the same specialized ribosome approach previously used for establishing the canonical SD-ASD interaction (17, 20, 23). Our findings do not support the discontinuous SD hypothesis. The effect of the conserved GGA on translation initiation must therefore be explained by other mechanisms, and plausible models are discussed. Interestingly, our data also

suggest that, under the conditions used here, specialized ribosomes are only moderately discriminated against for the translation of bulk cellular mRNA. The significance of this finding is discussed.

MATERIALS AND METHODS

Bacterial strains. The Lac$^-$ strain HfrG6Δ12 (11) was used for the construction of all chromosomal *rpsA-lacZ* and *galE-lacZ* fusions. This strain carries a short chromosomal deletion of the promoter and the RBS of the *lacZ* gene (nucleotides −52 to +20 [all numberings refer to the first base of the initiation codon]). Strains DH5α (*supE44* Δ*lac*U169(ϕ80 *lacZ*ΔM15) *hsdR17 recA1 endA1 gyrA96 thi-1 relA1*) or XL1-Blue (*supE44 hsdR17 recA1 endA1 gyrA46 thi relA1 lac* F′ [*proAB*$^+$ *lacI*^{q} *lacZ*ΔM15 Tn*10* (Tet^r)]) were used for plasmid propagation.

Construction of *rpsA-lacZ* and *galE-lacZ* translational fusions. Plasmid pES191 is a pEMBLΔ46 derivative (11) that carries a translational fusion between the wild-type *rpsA* TIR sequence (nucleotides −91 to +57) and the 5′ coding sequence of the *lacZ* gene (nucleotides +22 to +204) (3). This plasmid was used to introduce deletion and simple or multiple mutations in the *rpsA* TIR by using either DpnI mutagenesis (Stratagene) or PCR fusion mutagenesis with appropriate designed oligonucleotides. Combined mutations were introduced by successive mutagenesis of various pES191 derivatives. All resulting plasmids were checked by sequencing and then used to transfer the mutated *rpsA-lacZ* fusion onto the chromosome of HfrG6Δ12 by homologous recombination (11). The resulting HfrG6Δ12 derivatives were checked by sequencing of PCR-amplified chromosomal fragments encompassing the *rpsA-lacZ* fusion regions.

Similarly, plasmid pΔ46*galE*^{WT} is a pEMBLΔ46 derivative that carries a translational fusion between wild-type *galE* RBS sequence (nucleotides −35 to +28) and the 5′ coding sequence of the *lacZ* gene (43). Alteration of the *galE* SD from GGAG(C) to CCUCC was achieved by cloning two annealed oligonucleotides encompassing the *galE* RBS into appropriate BamHI and PstI sites of pEMBLΔ46 to yield pΔ46*galE*^{CCUCC}. Wild-type and mutated *galE-lacZ* fusions were transferred onto the chromosome of HfrG6Δ12 as described above.

Specialized ribosome system. The specialized ribosome system is carried by the kanamycin-resistant plasmids pOFX503 and pOFX504. These p15A derivatives (Kan^r) contain arabinose-inducible *rrnB* operons encoding 16S rRNA with wild-type (caCCUCCuua) or mutated (caGGAGGuua) anti-SD, respectively. Briefly, the *rrnB* operon was first cloned as three separate PCR fragments, and a restriction site was added after the end of the 16S rRNA gene to allow convenient substitutions in the anti-SD by using oligonucleotide cloning (details are available on request). Plasmids pOFX503 and pOFX504 were further modified by PCR fusion mutagenesis to introduce a C→T transition at position 1192 of the 16S rRNA, yielding pASD^{WT} and pASD^{mut}, respectively (Fig. 2A). The C1192T mutation confers spectinomycin resistance (38). These modified plasmids were checked by sequencing and used in all experiments.

Detection of plasmid-encoded 16S rRNA. The C1192T mutation was used to differentiate plasmid-encoded and chromosome-encoded 16S rRNA in total cellular RNA by using primer extension (38) (Fig. 3A and B). The strain containing the wild-type *galE-lacZ* chromosomal fusion was used for this purpose (no IPTG [isopropyl-β-D-thiogalactopyranoside] was added so that the fusion remains uninduced). Cells transformed with either the pASD^{WT} or pASD^{mut} plasmid were grown at 37°C in LB medium supplemented with kanamycin (50 μg/ml). After treatment with arabinose (0.2% final concentration) for the indicated time, cells were collected (optical density at 600 nm [OD_{600}] of 0.5 to 0.6) and total RNA was extracted with acidic phenol. For primer extension, 0.5 μg of total RNA was annealed with 0.2 pmol of γ-^{33}P-labeled A16S-1210 primer (5′-GGGCCATGATGACTTGA-3′). Reactions were performed in the presence of ddGTP (2.5 mM) instead of dGTP as described previously (38) so that extension stops at the positions indicated in Fig. 3A. After separation on a 12% polyacrylamide-urea gel, the radioactivity present in the 39- or 19-nt extension products (Fig. 3A and B) was quantified with a FLA3000 PhosphoFluoImager (Fuji) (Table 1).

Polysome profiles. Synthesis of specialized ribosomes was induced as described above, and cells were harvested 2 h after arabinose induction. Cell extracts were prepared as described previously (7). Ten OD_{260} units of extract was loaded onto 10 to 40%(wt/vol) sucrose gradients, spun at 35,000 rpm for 3 h in a Kontron TST41 rotor, and then analyzed with an ISCO UA-6 detector with continuous monitoring at 254 nm. Fractions (Fig. 3B) were collected, ethanol precipitated, and analyzed by primer extension.

Measurement of β-galactosidase activity. For measurement of β-galactosidase activity, cells were grown as described above and activity was assayed as described previously (2). Each measurement was done at least in triplicate. For each assay of ASD^{WT} or ASD^{mut} ribosomes, cultures were treated for at least 2 h with arabinose (0.2%), and then IPTG (500 μM) was added to induce the *lac* operon. Incubation was continued for an additional 30 min before harvesting of cells.

2D gel electrophoresis. Cells were grown in 20 ml of LB supplemented with arabinose (0.2%) and kanamycin (50 μg/ml) and harvested at an OD_{600} of 0.5. Pellets were treated with Bugbuster (Novagen) supplemented with Complete EDTA-free protein inhibitors (Roche), 1 unit/ml benzonase, and 400 μg/ml lysozyme, according to the manufacturer's protocol (Novagen). Soluble proteins (500 μg) were resuspended in 400 μl of solubilization buffer {8 M urea, 2% 3-[(3-cholamidopropyl)-dimethylammonio]-1-propanesulfonate (CHAPS), 40 mM dithiothreitol} and analyzed by two-dimensional (2D) gel electrophoresis (first dimension, Immobiline DryStrip, pH 4 to 7 [Amersham]; second dimension, 10% acrylamide-sodium dodecyl sulfate gel). Gels were stained with Coomassie blue G250 and scanned on a GS-800 imaging densitometer (Bio-Rad). Individual spots were quantified with PDQuest software for 2D analysis (Bio-Rad).

In vivo protein labeling. Cells were grown in M63 minimal medium (28) supplemented with vitamin B_1 (0.05%), histidine (0.01%), glycerol (0.9%), and kanamycin (50 μg/ml) to an OD_{600} of 0.15 to 0.2. Cultures were then supplemented with arabinose (0,2%) and, after 3 hours, with spectinomycin (500 μg/ml). Aliquots (0.5 ml) were labeled with 50 μCi of [^{35}S]Met/Cys (Pro-Mix; Amersham) either immediately or 30 min after spectinomycin addition. Labeling was stopped after 1 min with excess cold Met and Cys. Cells were harvested, lysed by sonication, and analyzed on a 10% NuPage gel (Invitrogen).

Lead(II) acetate probing of *rpsA* mRNA. Probing was performed on 157-nt-long, in vitro-transcribed RNA fragments encompassing the (loopI+II^{WT},AUG) (WT) or (loopI+II^{mut},AUG) *rpsA* TIRs. These fragments span nt −91 to +57 of the *rpsA* mRNA with a GGATCCGTC extension at the 5′ end. Templates for transcription were PCR amplified from pES191 or its (loopI+II^{mut},AUG) derivative, using primers 5′-TAATACGACTCACTATAGGATCCGTCCCCCGTTGC-3′ (upstream primer; the T7 RNA polymerase promoter is underlined) and 5′-GCGGGTTTCGATTTCTTTTAAGG-3′ (downstream primer). Transcription was carried out according to the Ambion MEGAshortscript protocol with [α-^{32}P]UTP as a tracer and guanosine (20 mM) as the initiator nucleotide. The latter allows subsequent RNA 5′ end labeling without dephosphorylation. RNA was gel purified, eluted, and resuspended in water; its concentration was estimated from the amount of ^{32}P incorporated. Ten picomoles of each transcript was then 5′ end labeled with [γ-^{33}P]ATP and subsequently purified on ProbQuantG50 microcolumns (Pharmacia). The protocol for lead(II)-mediated cleavage was adapted from published methods (18, 24). Briefly, cleavage was performed with 50,000 cpm of 5′-labeled RNA in the presence of 2 μg of yeast tRNA (Sigma) in 50 mM Tris acetate, 5 mM Mg-acetate, and 50 mM K-acetate. Prior to lead(II) acetate addition, labeled RNA was heated at 65°C for 5 min and then slowly (80 min) cooled to 20°C. Reactions were performed in a final volume of 10 μl for 10 min at 20°C and stopped by adding 1 μl of 0.5 M EDTA. Control samples were treated similarly but without lead(II). RNA was then precipitated and analyzed on an 8% polyacrylamide gel with 7 M urea. A ladder obtained by partial alkaline hydrolysis of the same RNA was run in parallel; for this purpose, labeled RNA (50,000 cpm) was incubated for 1 min at 90°C in 50 mM Na_2CO_3–50 mM $NaHCO_3$ (pH 9) in the presence of 2 μg yeast tRNA.

RESULTS

Overall design of the experimental system. Throughout this work, the translational activity of wild-type or mutated TIRs was quantified by monitoring the expression of β-galactosidase from suitable chromosomal fusions, as previously described (2, 43). Briefly, the region of the chromosome carrying the genuine *lacZ* TIR (from position −52 to +20 with respect to the first base of the initiator AUG) has been replaced by DNA fragments encompassing the TIRs of other genes (*galE* and *rpsA* in this work) so that β-galactosidase synthesis is driven at the transcription level by the *lac* promoter and at the translational level by the inserted TIR (Fig. 2A; see Materials and Methods).

The specialized ribosome system consists of two p15A-based plasmids (10 to 12 copies/cell) carrying the *rrnB* operon under

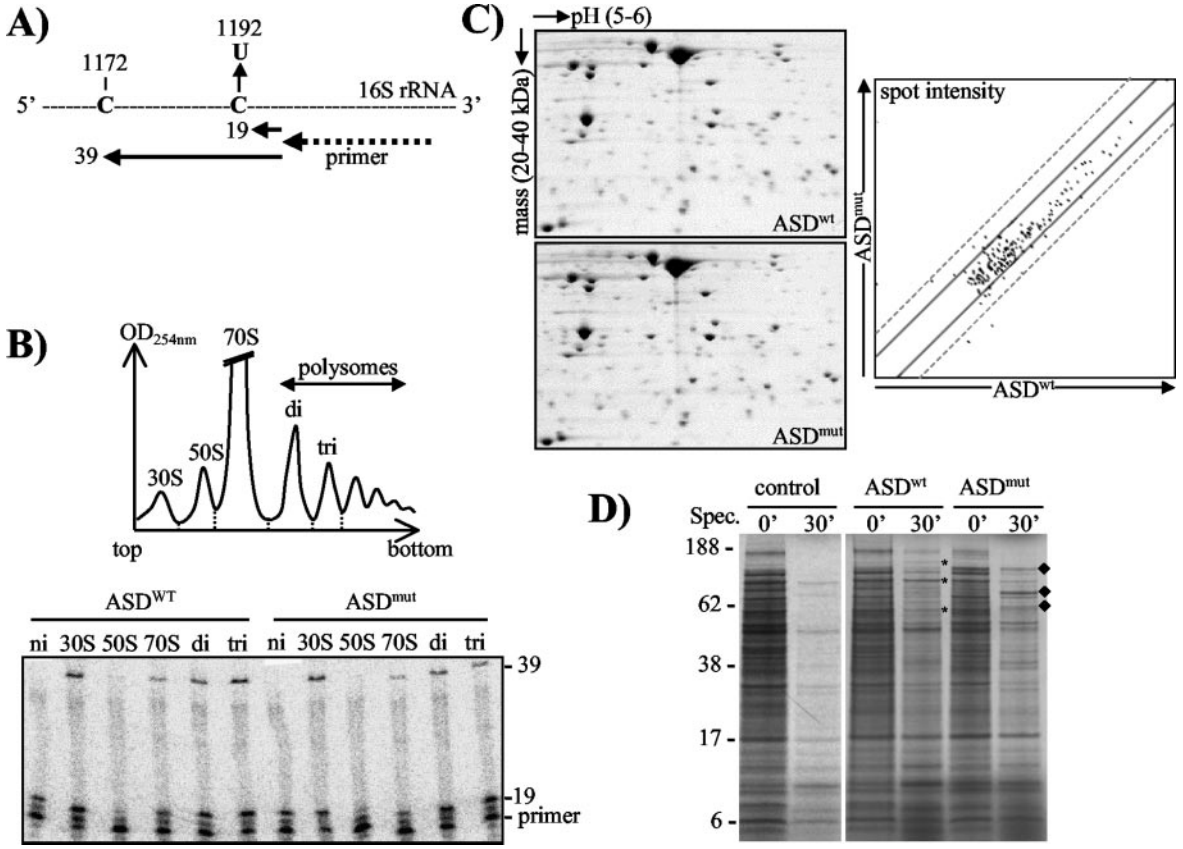

FIG. 3. Expression and translational activity of specialized ribosomes. (A) The plasmid-encoded rRNA, which carries the C1192U mutation, can be distinguished from chromosome-encoded rRNA by primer extension. The relevant 16S rRNA region is illustrated, together with the 17-mer used as a primer (dotted arrow). In the presence of ddGTP (see Materials and Methods), primer extension on chromosome and plasmid-encoded 16S rRNA yields an extra 19 or 39 nt, respectively. (B) Upper panel, polysome profile from cells growing in LB medium and expressing plasmid-derived ribosomes. Equivalent profiles were obtained for cells harboring either pASD^{WT} or pASD^{mut}. The 30S, 50S, 70S, and polysome peaks are indicated. Lower panel, primer extension analysis on equal amounts of RNAs from the fractions indicated on the profile. Quantification is presented in Table 1. ni, total RNA from cells in which the expression of plasmid-derived ribosomes was not induced. (C) Left panels, 2D electrophoresis of proteins from cells grown in LB medium and expressing rRNA from plasmid pASD^{WT} (upper panel) or pASD^{mut} (lower panel). Only parts of the gels are shown. Right panel, compared intensities of 178 Coomassie blue-stained spots from the two gels shown (abscissa, pASD^{WT}; ordinate, pASD^{mut}). The solid and dashed lines parallel to diagonal correspond to twofold and fourfold differences between the two gels, respectively. (D) Like ASD^{WT} ribosomes, ASD^{mut} ribosomes can translate bulk cellular mRNAs in the absence of cellular ribosomes, although the resulting protein pattern is not identical in both cases. Cells growing in minimal medium in the presence of arabinose were treated with spectinomycin (Spec.) and then pulse-chased with [^{35}S]methionine either immediately (0 min) or after 30 min. Asterisks and diamonds indicate proteins that are preferentially synthesized by ASD^{WT} or ASD^{mut} ribosomes, respectively. "Control" refers to cells carrying a pASD^{WT} derivative lacking the C1192T mutation conferring spectinomycin resistance. Molecular masses are given in kDa.

the control of an arabinose-inducible promoter (Fig. 2A). In one of them (hereafter referred to as pASD^{WT}), the anti-SD is wild type, whereas in the other (pASD^{mut}) it has been changed from **CCUCC**UUA-3′ to **GGAGG**UUA-3′ (Fig. 2A). Ribosomes containing the modified 16S rRNA should recognize the altered SD CCUCC. In order to tag plasmid-encoded rRNA within the ribosome population, a C→T transition was introduced in both plasmids at position 1192 of 16S rRNA (see Materials and Methods). This mutation, which also confers spectinomycin resistance, can be used to differentiate plasmid-encoded from chromosome-encoded 16S rRNA by primer extension (38) (Fig. 3A). For simplicity, "ASD^{WT}" and "ASD^{mut}" are used hereafter to designate rRNAs from plasmids pASD^{WT} and pASD^{mut}, respectively, or more generally for ribosomes or cells that contain these rRNAs. In contrast, "cellular" is used to designate chromosome-encoded 16S rRNA or the ribosomes that contain it.

TABLE 1. Distribution of plasmid-encoded 16S rRNA in the 30S subunit, the 70S particle, and polysomes

Plasmid	% Plasmid-encoded 16S rRNA (mean ± SD)[a]				
	Total	30S	70S	Disomes	Trisomes
pASD^{WT}	38 ± 3	38 ± 2	32 ± 0.5	31 ± 1	28 ± 2
pASD^{mut}	35 ± 4	33 ± 3	20 ± 7	16 ± 3	15 ± 0.5

[a] The percentage of plasmid-encoded 16S rRNA is taken as the ratio of the intensity of the +39 signal to the summed intensities of the +19 and +39 signals (see Fig. 3B). Cells were grown in LB medium and induced with arabinose for 3 h.

Specialized ribosomes can translate bulk cellular mRNA. To monitor the effect of specialized ribosomes on cell physiology, cells containing plasmid pASD^{WT} or pASD^{mut} were

grown in LB medium, and arabinose was added in log phase to induce expression of the plasmidic *rrnB* operon. After 2 h of induction, this expression, quantified by primer extension, reached a plateau corresponding to 35 to 38% of total 16S rRNA (Table 1); the value for ASD^{mut} rRNA is consistently slightly lower than for ASD^{WT}, perhaps indicating some instability of the former rRNA in vivo. Importantly, induction did not compromise steady-state growth. With ASD^{WT} rRNA the growth rate was unaffected, whereas with ASD^{mut} it was depressed by only ca. 10%, indicating that protein synthesis is not severely impaired (data not shown). To assess whether ASD^{mut} rRNA is incorporated into active ribosomes, its distribution into the 30S subunit, the 70S particle, and polysomes was determined. To this end, cell extracts were fractionated on sucrose gradients, and the 16S rRNA population from individual fractions was analyzed (Fig. 3A and B). As expected, the ASD^{WT} 16S rRNA was efficiently incorporated in polysomes; however, quantitatively, its relative abundance in polysomes was only 80% of that in 30S subunits (i.e., ca. 30/38) (Table 1), possibly indicating that, functionally, the C1192T mutation is not completely neutral (10, 35). Surprisingly, the ASD^{mut} 16S rRNA was also well represented in polysomes (Fig. 3B), with a proportion that reached ca. 45% of that in 30S subunits (i.e., 15/33) (Table 1). Obviously, ribosomes bearing ASD^{mut} are not strongly counterselected for translation, even though the cells contain no engineered mRNA with a complementary SD.

To determine whether ASD^{mut} ribosomes participate normally in cellular translation, protein extracts from ASD^{WT} or ASD^{mut} cells were compared by 2D gel electrophoresis (Fig. 3C). Quantification of 178 spots from Coomassie blue-stained gels showed that the two protein profiles were similar, with only 10% of the spots differing more than twofold in intensity between the two strains (Fig. 3C). The scarcity of ASD^{mut}-specific spots on the 2D gels suggests that ASD^{mut} ribosomes do not concentrate on a few specific mRNAs but participate in the translation of many, and perhaps most, well-translated cellular mRNAs.

The above conclusion seems at odd with previous work showing that ribosomes carrying mutated ASDs, including the ASD^{mut} sequence used here (system IX in reference 17) cannot translate cellular mRNAs normally (17, 20). A distinctive feature of these former studies compared to the present one is that the proportion of mutated versus cellular ribosomes was much higher. To test whether this higher proportion might explain the difference, we exploited the fact that in the presence of spectinomycin, cellular ribosomes are inactivated so that ASD^{WT} or ASD^{mut} ribosomes now constitute 100% of the ribosomes active in the cell. With the spectinomycin concentrations required to inhibit cellular ribosomes almost completely (i.e., 500 μg/ml), neither ASD^{WT} nor ASD^{mut} cells could achieve steady-state growth, perhaps because the concentration of spectinomycin-resistant ribosomes in the cell is insufficient. Nevertheless, protein synthesis in the two strains could be compared by adding the drug to growing cells and then pulse-labeling them with [^{35}S]methionine (see Materials and Methods). As expected, with ASD^{WT} cells, protein synthesis was reduced but still observable in the presence of the drug. Interestingly, the same hold true also for ASD^{mut} cells (Fig. 3D). Comparison of the two protein profiles shows a few individual species that are synthesized mainly or exclusively either by the ASD^{WT} or the ASD^{mut} ribosomes, together with a background that appears similar in the two cases (Fig. 3D). Altogether, quantification showed that, in the presence of spectinomycin, ^{35}S incorporation in ASD^{mut} cells was quite significant (ca. 50%) compared to that in ASD^{WT} cells, confirming that ASD^{mut} ribosomes can translate bulk cellular mRNAs.

In the past, specialized ribosomes have been assayed either under conditions illustrated above, i.e., moderate expression allowing steady-state growth (1, 23, 31), or under conditions of high expression and/or selective inactivation of cellular ribosomes, allowing only transient studies (5, 15, 17, 20). The former conditions have been preferred here, since steady-state conditions appear more physiologically relevant. Since ASD^{mut} ribosomes are then assayed in the presence of excess cellular ribosomes, their preferential utilization by a given TIR is detected as an increase in TIR activity over a nonzero background due to cellular ribosomes. Previously, this background has been taken as the activity of the TIR prior to induction of the specialized system (23, 31). For greater consistency, the activity of the TIR in the presence of ASD^{WT} ribosomes is used here for this purpose.

ASD^{mut} ribosomes preferentially translate an mRNA with a complementary SD. The specificity of the ASD^{mut} ribosomes was first evaluated with *lacZ* chromosomal fusions carrying the TIR from the *galE* gene. This particular TIR was chosen because its activity is stringently dependent upon the SD-ASD interaction (43). The *galE* SD, GGAG(C), was mutated to CCUCC, and strains carrying the wild-type or mutated *galE* TIR were then transformed with plasmid $pASD^{WT}$ or $pASD^{mut}$. After at least 2 hours of arabinose induction so that the concentration of plasmid-derived ribosomes reached a plateau, the *lac* operon was induced with IPTG and β-galactosidase expression was measured.

The activity of the wild-type *galE* TIR was high and was nearly identical whether ASD^{WT} or ASD^{mut} ribosomes were present (Fig. 4A). Concerning the mutant TIR, its activity was very low in the presence of ASD^{WT} ribosomes (ca. 1.5% of the wild-type value), consistent with the known stringency for SD-ASD interaction in this case. In the presence of ASD^{mut} ribosomes, this low activity was stimulated ~6-fold. Yet, activity still amounted to only 10% of the activity of the wild-type TIR. It is possible that compared with the wild-type TIR, the mutant TIR adopts a structure less favorable for ribosome binding. Alternatively, specialized ribosomes may be less efficient than the wild-type ribosomes for recognizing their cognate SD; one obvious reason is their lower concentration in the cytosol, which may not be enough to saturate the TIR. In any case, this experiment shows that the ASD^{mut} ribosomes can indeed recognize the modified SD, CCUCC.

The conserved GGA motifs in apical loops I and II of the *rpsA* TIR do not act as a discontinuous SD element. To test whether the conserved GGA motifs in the apical loops of hairpins I and II of the *rpsA* TIR constitute a discontinuous SD element, we simultaneously mutated them to CCU ($loopI+II^{mut}$,AUG in Fig. 1). Interestingly, this double replacement did not reduce the expression of the *rpsA-lacZ* fusion more than a single GGA→CCU replacement in loop I (result not shown) or than individual GG→AU replacements in either loop (3). The fact that alterations in either conserved

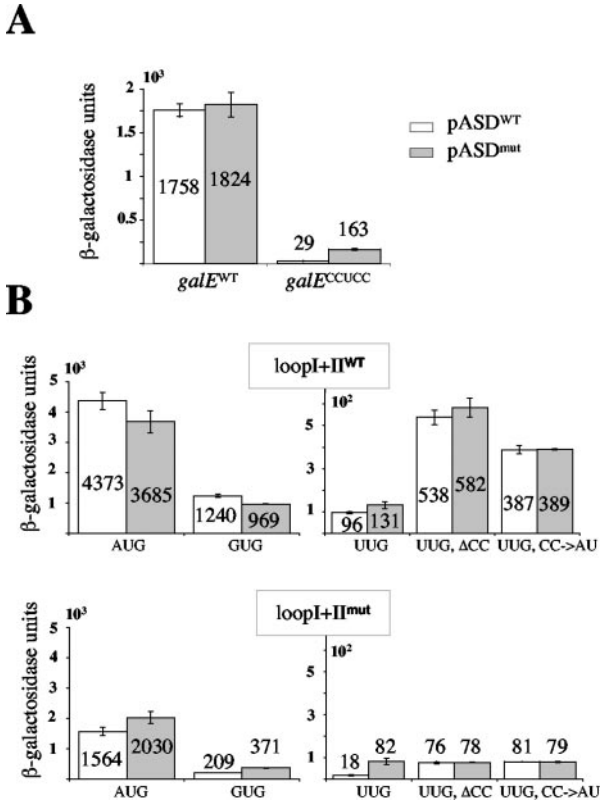

FIG. 4. Histograms showing β-galactosidase activities from the indicated TIR-*lacZ* translational fusions in the presence of ASD^{WT} or ASD^{mut} ribosomes. β-Galactosidase units correspond to nanomoles of *o*-nitrophenyl-β-D-galactopyranoside hydrolyzed per min and per mg of total protein. The values shown are averages from at least three independent assays. (A) β-Galactosidase expression from the $galE^{WT}$ and $galE^{CCUCC}$ TIRs. (B) β-Galactosidase expression from various mutants of the *rpsA* TIR. The different TIRs contain either the wild-type GGA motifs (loopI+II^{WT}) (upper panel) or the mutant CCU motifs (loopI+II^{mut}) (lower panel) in loops I and II, together with the indicated additional mutations (see Fig. 1). Note the different scales of individual histograms. Error bars indicate standard deviations.

GGA motif, or in both of them, affect translation to the same extent supports the view that these motifs work together for optimal TIR activity.

Plasmid $pASD^{WT}$ or $pASD^{mut}$ was then introduced into the strains carrying either the wild-type or the (loopI+II^{mut},AUG) TIR, and the activities of the TIRs were evaluated as described above. Like for the wild-type *galE* TIR, the activity of the wild-type *rpsA* TIR was not significantly different in the presence of either type of ribosome (Fig. 4B). In contrast, the activity of the (loopI+II^{mut},AUG) TIR was higher in the presence of the ASD^{mut} ribosomes, showing that the latter use the mutated TIR more efficiently than the ASD^{WT} ribosomes. Yet the effect (1.3-fold) was far more modest than that with the *galE* TIR (6-fold). An obvious reason for this smaller effect was that the (loopI+II^{mut},AUG) TIR still used wild-type ribosomes fairly efficiently; its activity in the presence of ASD^{WT} ribosomes was only threefold lower than that of the wild-type TIR. We therefore attempted to further manipulate the TIR so that its activity with wild-type ribosomes becomes more stringently dependent upon the presence of the GGA elements. To this end, the *rpsA* initiation codon was changed to GUG or UUG. The rationale here is that when the initiation codon is changed from an AUG to a non-AUG codon, the activity of the TIR generally becomes more dependent upon other elements, i.e., the SD or translational enhancers (34).

In the presence of ASD^{WT} ribosomes, changing the initiation codon AUG to GUG, and, even more so, to UUG, affected the activity of the TIR very negatively (by as much as 45-fold for UUG) (Fig. 4B). Importantly, this activity was now more dependent upon the presence of the GGA motifs in loops I and II; when the initiation codon was GUG or UUG, the introduction of the (loopI+II) mutation reduced TIR activity about sixfold, instead of threefold when the initiation codon was AUG (Fig. 4B). Like for the wild-type *rpsA* TIR, the presence of ASD^{mut} ribosomes had little effect on the activity of the (loopI+II^{WT},GUG) or (loopI+II^{WT},UUG) TIR. In contrast, when the loopI+II mutation was also present, ASD^{mut} ribosomes stimulated the TIR activity, as for the (loopI+II^{mut},AUG) TIR. However, stimulation was now larger: the (loopI+II^{mut},GUG) and (loopI+II^{mut},UUG) TIRs were stimulated 2- and 4.5-fold, respectively, versus 1.3-fold for the (loopI+II^{mut},AUG) TIR (Fig. 4B).

Whereas these results show that *rpsA* TIRs carrying the loopI+II mutation are preferentially recognized by ASD^{mut} ribosomes, they do not prove that this recognition reflects a pairing with the apical CCU motifs. Indeed, we noticed a possible slipped base pairing between the ASD^{mut} and the AACCU sequence present just before hairpin III, at nt −16 to −12 with respect to the initiator codon (Fig. 2B). To clarify the role of this sequence, we either deleted the CC doublet at nt −13 and −14 or replaced it by AU in the (loopI+II^{mut},UUG) TIR, for which the effect of specialized ribosomes was largest (ΔCC and CC→AU in Fig. 1 and 4B). As a control, the same mutations were also introduced in the (loopI+II^{wt},UUG) TIR. In all cases, in the absence of the ASD^{mut} ribosomes, alterations of the CC doublet significantly increased β-galactosidase synthesis, indicating that the CC doublet acts as a negative element in the *rpsA* TIR. More importantly, these alterations also completely abolished the stimulation of the (loopI+II^{mut},UUG) TIR by ASD^{mut} ribosomes (Fig. 4B). This result indicates that the observed stimulation reflects the presence of a spurious SD-like sequence that can pair with the ASD^{mut}; in its absence, the loopI+II-mutated TIR is not stimulated by ASD^{mut} ribosomes.

This lack of stimulation may reflect a conformational difference between the loopI+II^{WT} and loopI+II^{mut} TIRs that renders the CCU trinucleotides unavailable for pairing. However, the *mfold* algorithm (26, 45) predicts that the secondary structure of the *rpsA* TIR does not vary upon changing the GGA triplets to CCU. To further document this point, the in vitro structures of the wild-type and (loopI+II^{mut},AUG) TIRs were probed with lead(II). This reagent preferentially recognizes and cleaves single-stranded regions, largely independently of their sequence (18, 24). Consistent with theoretical predictions, this technique revealed no difference in structure between the wild-type and loopI+II^{mut} TIRs (Fig. 5). In particular, the CCU triplets appear to be fully accessible in the mutant.

Altogether, these experiments show that the conserved

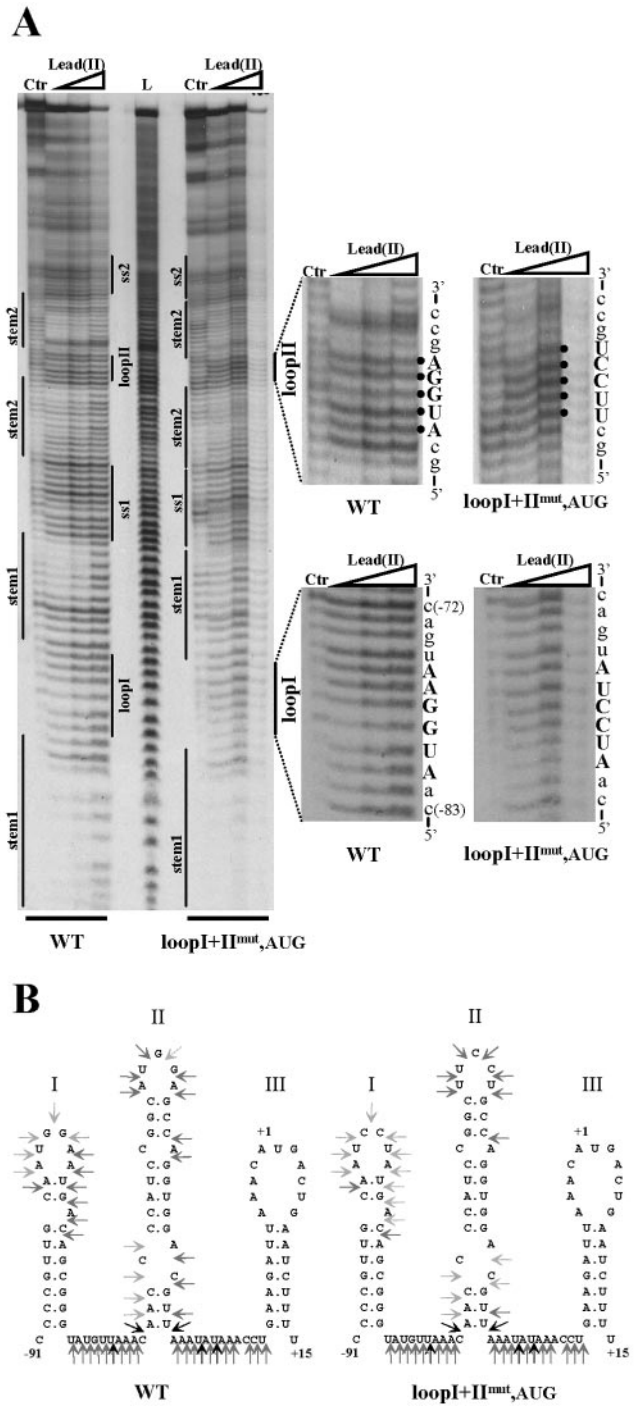

FIG. 5. Compared patterns of lead(II)-induced cleavages in *rpsA* TIRs carrying either loopI+II^{WT} or loopI+II^{mut} (Fig. 1). (A) In vitro-transcribed wild-type (WT) and (loopI+II^{mut},AUG) TIRs were probed with 60, 80, and 100 mM lead(II). Ctr, control without lead(II). L, alkaline hydrolysis ladder. Positions of the stem-and-loop regions of hairpins I and II and of single stranded regions (ss1 and ss2) are indicated. The smaller panels (right) focus on the apical loops of hairpins I and II; the relevant sequence is indicated on the right side, and uppercase is used for nucleotides from the loops. (B) The cleavage pattern of the region encompassing hairpins I and II is represented on the secondary structure model of the *rpsA* TIR (3). Strong, average, and weak cleavages are indicated by black, gray, and dotted arrows, respectively.

GGA motifs in loops I and II do not act as a discontinuous SD element.

DISCUSSION

The role of two conserved GGA motifs in the *rpsA* TIR. As noted in the introduction, the *rpsA* TIR is unique in being highly structured (Fig. 1) and in requiring this conserved structure for high translational activity (3). One possibility is that the structure serves to present sequence elements optimally for interaction with the 30S subunit during initiation. In particular, two conserved GGA motifs, located in apical loops I and II of the *rpsA* TIR, are required for maximal activity of the TIR, and chemical probing suggests that they are largely accessible for a possible interactions with the 30S subunit (Fig. 5) (3). Taking advantage of established specialized ribosome systems in *E. coli*, we have addressed the nature of this interaction here. Because the two GGA triplets resemble SD elements, we have targeted the anti-SD sequence of the 16S rRNA as the putative interacting site. These triplets were changed from GGA to CCU, a change that, depending upon the construct used, depresses the activity of the TIR three- to sevenfold (Fig. 4B) without perturbing its structure, as judged from theoretical predictions (45) and structure-probing experiments (Fig. 5). However, the symmetrical change of the ASD from CCUCC UUA-3′ (ASD^{WT}) to GGAGGUUA-3′ (ASD^{mut}) did not bring any specific stimulation of the mutated TIR, except for an adventitious SD-like stimulation involving an AACCU motif located 12 to 16 nt upstream of the *rpsA* initiation codon (Fig. 2B and 4B). As a control, when a similar change [GGAG(C) to CCUCC] was introduced into the SD of the *galE* TIR, which depends stringently upon its SD for activity, the residual activity was stimulated by ASD^{mut} ribosomes by as much as 600%. Altogether, the most straightforward interpretation of our data is that the two apical GGA motifs from loops I and II of the *rpsA* TIR do not form a discontinuous SD element, as initially proposed (3). Since the vestigial SD in stem III is also dispensable for activity (3), it seems plausible that the natural *rpsA* TIR does not rely at all upon an SD-ASD interaction for translation initiation.

Why, then, are the apical GGA motifs required for high translational activity? They may constitute interacting sites for regions of 16S rRNA other than the anti-SD or for a protein(s) from the translational machinery. Among the latter, one candidate is protein S1 itself. Ribosome-bound S1 is essential for the translation of most or all cellular mRNAs (39). Intriguingly, the RNA aptamer that binds S1 most tightly consists of a pseudoknot carrying a GGA motif in one of its loops (32). We speculate that, analogously, the GGA motifs from loops I and II may constitute recognition sites for ribosome-bound S1, allowing the correct positioning of the initiator codon to the P site. That purine-rich loops may constitute S1 binding sites has been suggested by others (40). Interestingly, the *rpsA* TIR is unique in that its activity is strongly repressed by free S1 (autoregulation) (2). Chemical protection analyses have identified ss1, ss2, and part of loop III as targets for free S1, but the binding sites of free S1 and ribosome-bound S1 may not coincide. The susceptibility of the GG residues from both loops I and II to chemical modification increases in the presence of free S1, suggesting that the loops then undergo a conforma-

tional change (3). Possibly, this conformational change prevents recognition of the TIR by ribosome-bound S1.

Specialized ribosomes can translate bulk cellular mRNA. Under the conditions used here, the ASD^{mut} 16S rRNA represents ca. 35% of total 16S rRNA, yet growth is not severely affected. This observation is consistent with that of Lee et al. (23), who found that cells expressing the same ASD^{mut} 16S rRNA at a level similar to that used here were viable (clone 6 in reference 23). We also found that the ASD^{mut} ribosomes are fairly efficiently enrolled in translation, even in the absence of a specific, complementary mRNA; their proportion in polysomes reaches 45% of their proportion in free 30S particles. Yet, the pattern of protein synthesized is similar to that observed in cells expressing the ASD^{WT} ribosomes. Together, these two results suggest that ASD^{mut} ribosomes participate in the translation of many cellular mRNAs and that, on the average, they are discriminated against by a factor of only about 2 in translation initiation. This observation was confirmed directly by using conditions where only ASD^{mut} ribosomes (or ASD^{WT} ribosomes) are active, i.e., in the presence of spectinomycin. Under these non-steady-state conditions, the patterns of protein synthesized by the ASD^{mut} and ADS^{WT} ribosomes were not identical, but quantitatively, protein synthesis by ASD^{mut} ribosomes was still about one-half of that for ASD^{WT} ribosomes.

How can ASD^{mut} ribosomes translate bulk cellular mRNAs in the absence of a cognate SD-ASD interaction? A fraction of these mRNAs may spuriously carry SD-like elements with complementarity to ASD^{mut}. The triplets ACC, UCC, and CCU all potentially bind the ASD^{mut} with significant free energy (-1.2 to -1.8 kcal/mol [13]). Assuming that these triplets are not discriminated against in natural TIRs, about 50% of the TIRs will, on a random basis, carry one of them 4 to 15 nt upstream of the initiation codon, i.e., in a position where it may act as a minimal SD towards ASD^{mut} ribosomes. As an illustration, the *rpsA* TIR itself carries an AACCU sequence that apparently can interact proficiently with ASD^{mut} ribosomes (Fig. 4B). Alternatively, it is possible that cellular ribosomes, when present in the cell together with ASD^{mut} ribosomes, can channel them into translation. Indeed, if an essential role of the SD-ASD interaction is to open inhibitory local secondary structures (8, 40), then after initiation by a ribosome with a wild-type ASD, opening may last long enough for ribosomes lacking such an ASD to initiate translation. Finally, it is possible that a significant fraction of all cellular mRNAs relies only marginally, if at all, on the SD-ASD interaction for translation, as exemplified here by the *rpsA* mRNA itself. Such mRNAs would make no distinction between wild-type and specialized ribosomes. There is, in fact, much evidence supporting the view that the SD-ASD interaction is not always required for efficient translation. In vitro, this interaction is clearly dispensable (6, 27). In vivo, our observation that translation of bulk cellular mRNAs remains significant when only ASD^{mut} ribosomes are active in the cell is not unprecedented (15, 17; see Fig. 5, lanes 6 to 8, in reference 17), although this point was not emphasized in these previous studies. Other arguments support the idea that SD-independent translation is not marginal in *E. coli*. Although highly expressed genes generally possess stronger SDs than average ones, as many as 12% of *E. coli* mRNAs lack a recognizable SD (25). Consistent with the dispensability of the SD interaction, artificial mRNAs lacking an SD in their leader sequences (42), and even leaderless mRNAs (22), can be translated in *E. coli*. Even for TIRs with a bona fide SD, cases are known where alterations in the SD do not abrogate or even do not affect activity, in spite of the loss of the SD-ASD interaction (12, 19, 23). Thus, the situations exemplified here with the *galE* and *rpsA* TIRs (stringent dependence or no dependence upon the SD-ASD interaction, respectively) may simply constitute extreme cases of a more common situation where the SD-ASD interaction is only one element among others contributing to translation initiation.

ACKNOWLEDGMENTS

We are indebted to Irina Boni (Russian Academy of Sciences, Moscow, Russia) for having initiated studies on the *rpsA* TIR in our laboratory. We thank Eliane Hajnsdorf (IBPC, Paris, France) and Pascale Romby (IBMC, Strasbourg, France) for their valuable advice on RNA probing experiments.

This work is supported by the Centre National de la Recherche Scientifique, by the École Normale Supérieure, and by the Agence Nationale pour la Recherche (grant NT05-1_44659) to M.D. and by fellowships from the French Ministère de l'Éducation Nationale de l'Enseignement Supérieur et de la Recherche (MENESR) and the Fondation pour la Recherche Médicale (FRM) to P.S.

REFERENCES

1. **Bélanger, F., M. Léger, A. A. Saraiya, P. R. Cunningham, and L. Brakier-Gingras.** 2002. Functional studies of the 900 tetraloop capping helix 27 of 16S ribosomal RNA. J. Mol. Biol. **320:**979–989.
2. **Boni, I. V., V. S. Artamonova, and M. Dreyfus.** 2000. The last RNA-binding repeat of the *Escherichia coli* ribosomal protein S1 is specifically involved in autogenous control. J. Bacteriol. **182:**5872–5879.
3. **Boni, I. V., V. S. Artamonova, N. V. Tzareva, and M. Dreyfus.** 2001. Non-canonical mechanism for translational control in bacteria: synthesis of ribosomal protein S1. EMBO J. **20:**4222–4232.
4. **Boni, I. V., D. M. Isaeva, M. L. Musychenko, and N. V. Tzareva.** 1991. Ribosome-messenger recognition: mRNA target sites for ribosomal protein S1. Nucleic Acids Res. **19:**155–162.
5. **Brink, M. F., G. Brink, M. P. Verbeet, and H. A. de Boer.** 1994. Spectinomycin interacts specifically with the residues G1064 and C1192 in 16S rRNA, thereby potentially freezing this molecule into an inactive conformation. Nucleic Acids Res. **22:**325–331.
6. **Calogero, R. A., C. L. Pon, M. A. Canonaco, and C. O. Gualerzi.** 1988. Selection of the mRNA translation initiation region by *Escherichia coli* ribosomes. Proc. Natl. Acad. Sci. USA **85:**6427–6431.
7. **Charollais, J., D. Pflieger, J. Vinh, M. Dreyfus, and I. Iost.** 2003. The DEAD-box RNA helicase SrmB is involved in the assembly of 50S ribosomal subunits in *Escherichia coli*. Mol. Microbiol. **48:**1253–1265.
8. **de Smit, M. H., and J. van Duin.** 1994. Translational initiation on structured messengers. Another role for the Shine-Dalgarno interaction. J. Mol. Biol. **235:**173–184.
9. **de Smit, M. H., and J. van Duin.** 1990. Secondary structure of the ribosome binding site determines translation efficiency: a quantitative analysis. Proc. Natl. Acad. Sci. USA **87:**7668–7672.
10. **Dragon, F., C. Spickler, R. Pinard, J. Carrière, and L. Brakier-Gringas.** 1996. Mutations of non-canonical base-pairs in the 3′ major domain of *Escherichia coli* 16 S ribosomal RNA affect the initiation and elongation of protein synthesis. J. Mol. Biol. **259:**207–215.
11. **Dreyfus, M.** 1988. What constitutes the signal for the initiation of protein synthesis on *Escherichia coli* mRNAs? J. Mol. Biol. **204:**79–94.
12. **Fargo, D. C., M. Zhang, N. W. Gillham, and J. E. Boynton.** 1998. Shine-Dalgarno-like sequences are not required for translation of chloroplast mRNAs in *Chlamydomonas reinhardtii* chloroplasts or in *Escherichia coli*. Mol. Gen. Genet. **257:**271–282.
13. **Freier, S. M., R. Kierzek, J. A. Jaeger, N. Sugimoto, M. H. Caruthers, T. Neilson, and D. H. Turner.** 1986. Improved free-energy parameters for predictions of RNA duplex stability. Proc. Natl. Acad. Sci. USA **83:**9373–9377.
14. **Gold, L.** 1988. Posttranscriptional regulatory mechanisms in *Escherichia coli*. Annu. Rev. Biochem. **57:**199–233.
15. **Govantes, F., E. Andujar, and E. Santero.** 1998. Mechanism of translational coupling in the nifLA operon of *Klebsiella pneumoniae*. EMBO J. **17:**2368–2377.
16. **Hartz, D., D. S. McPheeters, and L. Gold.** 1991. Influence of mRNA determinants on translation in *Escherichia coli*. J. Mol. Biol. **218:**83–97.

17. **Hui, A., and H. A. de Boer.** 1987. Specialized ribosome system: preferential translation of a single mRNA species by a subpopulation of mutated ribosomes in *Escherichia coli*. Proc. Natl. Acad. Sci. USA **84:**4762–4766.
18. **Huntzinger, E., M. Possedko, F. Winter, H. Moine, C. Ehresmann, and P. Romby.** 2005. Probing RNA structure with enzymes and chemicals *in vitro* and *in vivo*, p. 151–170. *In* R. K. Hartmann, A. Bindereif, A. Schön, and E. Westhof (ed.), Handbook of RNA biochemistry. Wiley-VCH Verlag GmbH and Co., Weinheim, Germany.
19. **Inokuchi, Y., A. Hirashima, Y. Sekine, L. Janosi, and A. Kaji.** 2000. Role of ribosome recycling factor (RRF) in translational coupling. EMBO J. **19:** 3788–3798.
20. **Jacob, W. F., M. Santer, and A. E. Dahlberg.** 1987. A single base change in the Shine-Dalgarno region of 16S rRNA of *Escherichia coli* affects translation of many proteins. Proc. Natl. Acad. Sci. USA **84:**4757–4761.
21. **Jenner, L., P. Romby, B. Rees, C. Schulze-Briese, M. Springer, C. Ehresmann, B. Ehresmann, D. Moras, G. Yusupova, and M. Yusupov.** 2005. Translational operator of mRNA on the ribosome: how repressor proteins exclude ribosome binding. Science **308:**120–123.
22. **Laursen, B. S., H. P. Sorensen, K. K. Mortensen, and H. U. Sperling-Petersen.** 2005. Initiation of protein synthesis in bacteria. Microbiol. Mol. Biol. Rev. **69:**101–123.
23. **Lee, K., C. A. Holland-Staley, and P. R. Cunningham.** 1996. Genetic analysis of the Shine-Dalgarno interaction: selection of alternative functional mRNA-rRNA combinations. RNA **2:**1270–1285.
24. **Lindell, M., P. Romby, and E. G. Wagner.** 2002. Lead(II) as a probe for investigating RNA structure *in vivo*. RNA **8:**534–541.
25. **Ma, J., A. Campbell, and S. Karlin.** 2002. Correlations between Shine-Dalgarno sequences and gene features such as predicted expression levels and operon structures. J. Bacteriol. **184:**5733–5745.
26. **Mathews, D. H., J. Sabina, M. Zuker, and D. H. Turner.** 1999. Expanded sequence dependence of thermodynamic parameters improves prediction of RNA secondary structure. J. Mol. Biol. **288:**911–940.
27. **Melançon, P., D. Leclerc, N. Destroismaisons, and L. Brakier-Gingras.** 1990. The anti-Shine-Dalgarno region in *Escherichia coli* 16S ribosomal RNA is not essential for the correct selection of translational starts. Biochemistry **29:**3402–3407.
28. **Miller, J. H.** 1972. Experiments in molecular genetics. Cold Spring Harbor Laboratory, Cold Spring Harbor, N.Y.
29. **Nakamoto, T.** 2006. A unified view of the initiation of protein synthesis. Biochem. Biophys. Res. Commun. **341:**675–678.
30. **Nivinskas, R., N. Malys, V. Klausa, R. Vaiskunaite, and E. Gineikiene.** 1999. Post-transcriptional control of bacteriophage T4 gene 25 expression: mRNA secondary structure that enhances translational initiation. J. Mol. Biol. **288:** 291–304.
31. **Praszkier, J., and A. J. Pittard.** 2002. Pseudoknot-dependent translational coupling in *repBA* genes of the IncB plasmid pMU720 involves reinitiation. J. Bacteriol. **184:**5772–5780.
32. **Ringquist, S., T. Jones, E. E. Snyder, T. Gibson, I. Boni, and L. Gold.** 1995. High-affinity RNA ligands to *Escherichia coli* ribosomes and ribosomal protein S1: comparison of natural and unnatural binding sites. Biochemistry **34:**3640–3648.
33. **Ringquist, S., M. MacDonald, T. Gibson, and L. Gold.** 1993. Nature of the ribosomal mRNA track: analysis of ribosome-binding sites containing different sequences and secondary structures. Biochemistry **32:**10254–10262.
34. **Ringquist, S., S. Shinedling, D. Barrick, L. Green, J. Binkley, G. D. Stormo, and L. Gold.** 1992. Translation initiation in *Escherichia coli*: sequences within the ribosome-binding site. Mol. Microbiol. **6:**1219–1229.
35. **Rodriguez-Correa, D., and A. E. Dahlberg.** 2004. Genetic evidence against the 16S ribosomal RNA helix 27 conformational switch model. RNA **10:** 28–33.
36. **Sacerdot, C., J. Caillet, M. Graffe, F. Eyermann, B. Ehresmann, C. Ehresmann, M. Springer, and P. Romby.** 1998. The *Escherichia coli* threonyl-tRNA synthetase gene contains a split ribosomal binding site interrupted by a hairpin structure that is essential for autoregulation. Mol. Microbiol. **29:** 1077–1090.
37. **Sengupta, J., R. K. Agrawal, and J. Frank.** 2001. Visualization of protein S1 within the 30S ribosomal subunit and its interaction with messenger RNA. Proc. Natl. Acad. Sci. USA **98:**11991–11996.
38. **Sigmund, C. D., M. Ettayebi, A. Borden, and E. A. Morgan.** 1988. Antibiotic resistance mutations in ribosomal RNA genes of *Escherichia coli*. Methods Enzymol. **164:**673–690.
39. **Sorensen, M. A., J. Fricke, and S. Pedersen.** 1998. Ribosomal protein S1 is required for translation of most, if not all, natural mRNAs in *Escherichia coli in vivo*. J. Mol. Biol. **280:**561–569.
40. **Studer, S. M., and S. Joseph.** 2006. Unfolding of mRNA secondary structure by the bacterial translation initiation complex. Mol. Cell **22:**105–115.
41. **Tchufistova, L. S., A. V. Komarova, and I. V. Boni.** 2003. A key role for the mRNA leader structure in translational control of ribosomal protein S1 synthesis in gamma-proteobacteria. Nucleic Acids Res. **31:**6996–7002.
42. **Tsareva, N. V., V. I. Makhno, and I. V. Boni.** 1994. Ribosome-messenger recognition in the absence of the Shine-Dalgarno interactions. FEBS Lett. **337:**189–194.
43. **Yarchuk, O., N. Jacques, J. Guillerez, and M. Dreyfus.** 1992. Interdependence of translation, transcription and mRNA degradation in the *lacZ* gene. J. Mol. Biol. **226:**581–596.
44. **Zhang, J., and M. P. Deutscher.** 1992. A uridine-rich sequence required for translation of prokaryotic mRNA. Proc. Natl. Acad. Sci. USA **89:**2605–2609.
45. **Zuker, M.** 2003. Mfold web server for nucleic acid folding and hybridization prediction. Nucleic Acids Res. **31:**3406–3415.